Distribution Kinetics Model for the Sol−Gel Transition Critical Exponent

Rujun Li

School of Chemical & Biomolecular Engineering, Georgia Institute of Technology, 311 Ferst Drive, Atlanta, Georgia 30332

Benjamin J. McCoy*

Department of Chemical Engineering, Louisiana State University, Baton Rouge, Louisiana 70803-7303

Received April 5, 2005; Revised Manuscript Received May 20, 2005

ABSTRACT: The pregelation weight-average molecular weights of cross-linked polymers and silica-based sol−gels diverge at the sol−gel transition, where time t approaches the gel time t_c. The divergence follows a power law, $(1 - t/t_c)^{-\gamma}$, with a critical exponent larger than the $\gamma = 1$ prediction of classic Flory−Stockmayer theory and of our previous cross-linking model. In this paper we modify the cross-linking mechanism by allowing a fractional exponent, $0 < \omega \leq 1$, for the mass-dependent rate kernel to match the critical exponents of real systems. Moment equations solved by closure approximations show that γ is determined solely by ω, in agreement with an existing analytical solution. The rate constants for cross-linking, addition, and condensation polymerization have essentially no effect on γ. We also obtained for the first time an analytical expression for gel time, in agreement with moment closure solutions for values of ω other than 0 or 1. When ω is either 3/4 or 5/6, good approximations to experimental values of γ for silica sol−gel or polymer, respectively, are found.

Introduction

The classic Flory[1] and Stockmayer[2] statistical theory of cross-linking pioneered the study of polymer networks and gels. The theory explained that in the sol−gel transition process, as time t approaches the gel time t_c, polymer properties such as weight-average molecular weight $\bar{M}_w$ diverge according to[3]

$$\bar{M}_w(t) = \bar{M}_w(0)\left(1 - \frac{t}{t_c}\right)^{-\gamma} \tag{1}$$

with $\gamma = 1$. For experimental polymer and sol−gel transitions, the power-law relationship is found to be true, diverging with an exponent γ greater than 1.[4] For most polymerizations, γ is between 1.5 and 1.8. For silica-based sol−gel the value is even larger, about 2.7.[5,6] Percolation theory,[7] contrary to the classic result, predicts $\gamma = 1.76$, in agreement with the measured γ for polymer gelation. The kinetic gelation model,[8−10] based on the Monte Carlo method applied to kinetic growth, predicts $\gamma = 2$.[9,10]

We previously studied the intermolecular cross-linking mechanism where two macromolecules cross-link through pendant functional groups or cross-linking agents and form a polymer network[11]

$$P_i(x) + P_j(x') \xrightarrow{k} P_{i+j+1}(x + x') \tag{2}$$

where $P_i(x)$ is a polymer with mass x and i cross-links and k is the rate coefficient. Using continuous distribution kinetics with a general mass-dependent rate kernel

$$k = \kappa(xx')^{\omega} \tag{3}$$

where κ is a constant and ω is a integer, we showed that if $\omega = 0$, gel will never form. If $\omega = 1$, however, gel forms when time approaches the critical time $t_c = 1/[2\kappa p^{[0](2)}(0)]$. This critical point is based on the first and second mass moments, $p^{[0](1)}$ and $p^{[0](2)}$, in the pregel region expressed as

$$p^{[0](1)}(t) = p^{[0](1)}(0) \tag{4}$$

$$p^{[0](2)}(t) = \frac{p^{[0](2)}(0)}{1 - 2\kappa t p^{[0](2)}(0)} \tag{5}$$

The ratio of eq 5 to eq 4 is the weight-average molecular weight (eq 1) with $\gamma = 1$, the same result as Flory's statistical approach.[1]

The objective of this paper is to extend the previous intermolecular cross-linking mechanism for polymerization and sol−gel processes to predict γ for ω different from 0 and 1 and to study the dependence of sol−gel transition on the ω value. We derive the analytical solution for the gel time t_c and examine the relations of γ, t_c and reaction conditions. In the Kinetics section the kinetics of sol−gel and cross-linking reactions are mathematically described via population balance equations and their moments. Because moment equations lack closure for ω different from 0 or 1, the section on moment closures describes approximations for solving the equations. Results are then discussed, and conclusions are drawn.

Mechanism

First we consider a general sol−gel polycondensation process. The silica-based sol−gel process includes steps of hydrolysis and condensation:[6]

hydrolysis

$$Si(OR)_4 + nH_2O \rightarrow Si(OR)_{4-n}(OH)_n + nROH \tag{6}$$

* To whom correspondence should be addressed. Present address: Department of Chemical Engineering and Materials Science, University of California, Davis, CA 95616. Phone: 530-752-0400. Fax: 530-752-1031. E-mail: bjmccoy@ucdavis.edu.

10.1021/ma050707b CCC: $30.25
Published on Web 06/28/2005

condensation

$$\gtrdot\text{SiOH} + \text{ROSi}\lessdot \rightarrow \gtrdot\text{SiOSi}\lessdot + \text{ROH} \quad (7)$$

$$\gtrdot\text{SiOH} + \text{HOSi}\lessdot \rightarrow \gtrdot\text{SiOSi}\lessdot + \text{H}_2\text{O} \quad (8)$$

The symbols $\gtrdot$ and $\lessdot$ represent three chemical bonds of tetravalent Si. The first step, hydrolysis, is fast compared to the condensation reactions;[12] therefore, we can assume the concentration of the monomer, $Si(OR)_{4-n}(OH)_n$, $1 \le n \le 4$, equals the concentration of silicon alkoxide, $Si(OR)_4$, if water is in excess. The second step can be further divided into three reactions: monomer addition, condensation, and cross-linking. Here we distinguish between condensation, a reaction between the ends of two polymers, and cross-linking, a reaction within either or both polymers.

When all monomers have the same reactivity, we can simplify the kinetics to a typical polymerization involving monomer addition (or propagation), condensation (or combination), and cross-linking. Because we are concerned about the evolution of mass-related bulk properties, such as weight-average molecular weight, rather than cross-link related properties, we can simplify our notation and define $P(x)$ as a macromolecule with molecular weight x and $M(x_m)$ as monomer of molecular weight x_m. The main reactions are then represented as

$$\text{monomer addition: } \text{P}(x) + \text{M}(x_m) \xrightarrow{k_p} \text{P}(x + x_m) \quad (9)$$

$$\text{condensation or chain combination: } \text{P}(x) + \text{P}(x') \xrightarrow{k_{cd}} \text{P}(x + x') \quad (10)$$

$$\text{intermolecular cross-linking: } \text{P}(x) + \text{P}(x') \xrightarrow{k} \text{P}(x + x') \quad (11)$$

In earlier work we studied and computed inter-[11] and intramolecular[13] cross-linking effects. Because intramolecular cross-linking does not affect mass moments and related properties, it is not considered in this work.

Kinetics

We use the rate kernel for intermolecular cross-linking[11] shown in eq 3 and assume k_p and k_{cd} are independent of polymer masses. The condensation involves functional groups at branch ends, while the cross-linking reaction involves functional groups within branches; thus, condensation is proportional to the number of chains, and cross-linking is proportional to the total number of functional groups, or mass. When the masses of polymers are large, the number of functional groups within branches is much larger than that at the end of branches; thus, condensation can be neglected. We define $p(x,t)\,dx$ as the concentration of polymer chains at time t with molecular weight in the range $(x, x + dx)$ and $m^{(0)}$ as the monomer concentration. The population balance equation for $p(x,t)$ in a batch reactor is[11]

$$\frac{\partial p(x,t)}{\partial t} = -2p(x)\int_0^\infty k(x,x')\,p(x')\,dx' + \int_0^x k(x', x - x')\,p(x - x')\,p(x')\,dx' - 2k_{cd}p(x)\int_0^\infty p(x')\,dx' + k_{cd}\int_0^x p(x - x')\,p(x')\,dx' + k_p m^{(0)}[p(x - x_m) - p(x)]$$

$$= -2\kappa x^\omega p(x)p^{(\omega)} + \kappa\int_0^x x'^\omega (x - x')^\omega p(x - x')\,p(x')\,dx' - 2k_{cd}p(x)p^{(0)} + k_{cd}\int_0^x p(x - x')\,p(x')\,dx' + k_p m^{(0)}[p(x - x_m) - p(x)] \quad (12)$$

where x_m is the monomer mass. The small mass loss due to the formation of water or alcohol (ROH) is neglected. The bulk moment is defined as

$$p^{(n)} = \int_{x=0}^\infty x^n p(x)\,dx \quad (13)$$

where n is the order of the mass moment. Applying the moment operation (eq 13) to eq 12 yields the governing equation for the bulk moments

$$\frac{dp^{(n)}}{dt} = -2\kappa p^{(n+\omega)}p^{(\omega)} + \kappa\sum_{h=0}^n \binom{n}{h} p^{(\omega+h)}p^{(\omega+n-h)} - 2k_{cd}p^{(n)}p^{(0)} + k_{cd}\sum_{h=0}^n \binom{n}{h} p^{(h)}p^{(n-h)} + k_p m^{(0)}\left[\sum_{i=0}^n \binom{n}{i} {x_m}^{n-i} p^{(i)} - p^{(n)}\right] \quad (14)$$

The expression collapses to the much discussed Smoluchowski's equation when $k_{cd} = k_p = 0$. The $n = 0$, 1, 2 mass moment equations follow from eq 14

$$\frac{dp^{(0)}}{dt} = -\kappa(p^{(\omega)})^2 - k_{cd}(p^{(0)})^2 \quad (15)$$

$$\frac{dp^{(1)}}{dt} = k_p m^{(0)} x_m p^{(0)} \quad (16)$$

$$\frac{dp^{(2)}}{dt} = k_p m^{(0)}[(x_m)^2 p^{(0)} + 2x_m p^{(1)}] + 2\kappa(p^{(1+\omega)})^2 + 2k_{cd}(p^{(1)})^2 \quad (17)$$

where $p^{(0)}$ and $p^{(1)}$ are the molar and mass concentrations of the polymer, respectively. The monomer moment equation from a mass balance is

$$\frac{dm^{(0)}}{dt} = -k_p m^{(0)} p^{(0)} \quad (18)$$

Combining eqs 16 and 18 yields the total mass balance $d(m^{(0)}x_m + p^{(1)})/dt = 0$. For ω equal to 0 or 1, the moment equations have been solved previously.[11] For ω different from 0 or 1, a closure approximation is required for $p^{(\omega)}$ and $p^{(1+\omega)}$ in the zeroth and second mass moment equations, eqs 15 and 17, respectively.

Moment Closures

When the molecular weight distribution (MWD) is a given function, the expressions for moments of all orders are related. For instance, for a Γ distribution

$$p(x) = \frac{\left(\frac{x}{\beta}\right)^{\alpha-1} e^{-x/\beta}}{\beta\Gamma(\alpha)} p^{(0)} \quad (19)$$

the mass moment for any $i \ge 0$ is

$$p^{(i)} = \int_0^\infty x^i p(x)\,dx = \beta^i \frac{\Gamma(\alpha + i)}{\Gamma(\alpha)} p^{(0)} \tag{20}$$

in terms of the gamma function Γ. The parameters α and β are computed from the $n = 0$, 1, and 2 mass moments:

$$\alpha = \frac{1}{\dfrac{\bar{M}_w}{\bar{M}_n} - 1} \tag{21}$$

$$\beta = \bar{M}_w - \bar{M}_n \tag{22}$$

where $\bar{M}_w = p^{(2)}/p^{(1)}$ and $\bar{M}_n = p^{(1)}/p^{(0)}$. For $i = 3$ the expression is

$$p^{(3)} = 2\frac{[p^{(2)}]^2}{p^{(1)}} - \frac{p^{(2)}}{p^{(0)}} p^{(1)} \tag{23}$$

If we assume the polymer follows a log−normal distribution, then

$$p(x) = \frac{p^{(0)}}{x\sigma\sqrt{2\pi}} e^{-(\ln x - \ln x_0^2/2\sigma)^2} \tag{24}$$

where $p^{(0)} = 1$ for a standard log−normal distribution. If we substitute ln x with y, then we can derive the ith moment

$$p^{(i)} = x_0^i e^{i^2\sigma^2/2} p^{(0)} \tag{25}$$

with

$$x_0 = \frac{\bar{M}_n}{\sqrt{p^{pd}}} \tag{26}$$

$$\sigma = \sqrt{\ln p^{pd}} \tag{27}$$

in terms of the number-average molecular weight $\bar{M}_n$ and the polydispersity $p^{pd} = \bar{M}_w/\bar{M}_n$. The moments can be expressed in terms of $n = 0$, 1, and 2 mass moment properties

$$p^{(i)} = (\bar{M}_n)^i (p^{pd})^{(i^2-i)/2} p^{(0)} \tag{28}$$

For $i = 3$ the expression is quite simple

$$p^{(3)} = \left[\frac{p^{(2)}}{p^{(1)}}\right]^3 p^{(0)} \tag{29}$$

A distribution function closure approach assumes that the MWD follows a particular distribution function at any time, with time-dependent parameters. The fractional moments, $p^{(\omega)}$ and $p^{(1+\omega)}$ in eqs 15 and 17, can be expressed by the first three integer moments, as in eq 20 for Γ closure and eq 28 for log−normal closure. Typically, Γ and log−normal distributions are used not only in closure approximations but also in reconstruction of MWDs.[14−16] There are other closures that do not assume a particular distribution function. The method of moments with interpolative closure (MOMIC)[17,18] is based on a polynomial for i to approximate the ith mass moment, $p^{(i)}$. For a second-order polynomial, the closure reduces to the log−normal distribution. The quadrature method of moments (QMOM)[19] uses N abscissas (L_k) and weightings (w_k) derived from the first $2N$ integer mass moments to approximate the ith mass moment, $p^{(i)}$

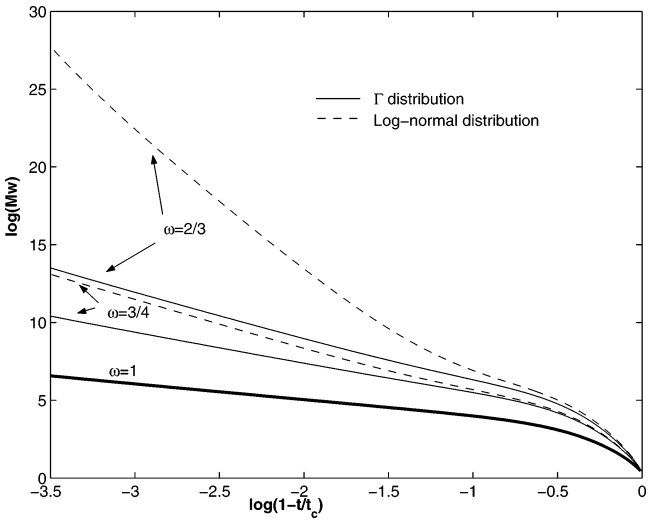

Figure 1. Dynamics of $\bar{M}_w$ with different ω.

$$p^{(i)} = \sum_{k=1}^{N} w_k L_k^{\,i} \tag{30}$$

Simulation results for the cross-linking reactions using a fifth-order MOMIC and a QMOM with $N = 5$ show that neither MOMIC nor QMOM can produce a smooth curve or show the pronounced straight line in the log($\bar{M}_w$) vs log($1 - t/t_c$) plot. Therefore, in this paper, we use the distribution function-based closure approach and evaluate the errors caused by Γ and log−normal closures.

Results and Discussion

Various simulations were conducted to test the effects of kinetic parameters on γ. The initial MWD of the polymer was considered an exponential distribution, $p(x) = p^{(0)}e^{-x/\beta}$, where β, the number-average molecular weight, is set to unity. Figure 1 is a plot of log($\bar{M}_w$) vs log($1 - t/t_c$) for large values of k_p and k_{cd} and a small value of κ to illustrate the effects of k_p and k_{cd}. Simulation results of both Γ and log−normal closures show the pronounced straight lines (Figure 1), whose slopes are determined solely by the ω value; i.e., κ and initial MWDs have no effect. Addition (k_p) and condensation (k_{cd}) reactions affect only the curve shape at the beginning of the reaction ($t \ll t_c$). The critical exponent of the sol−gel transition can be studied, therefore, by setting $k_p = k_{cd} = 0$ and choosing any value, e.g., unity, for κ. Then eq 12 becomes a standard Smoluchowski equation that has been studied extensively. The moment equations (eqs 15−17) are simplified as

$$\frac{dp^{(0)}}{dt} = -\kappa(p^{(\omega)})^2 \tag{31}$$

$$\frac{dp^{(1)}}{dt} = 0 \tag{32}$$

$$\frac{dp^{(2)}}{dt} = 2\kappa(p^{(1+\omega)})^2 \tag{33}$$

For large x as time t approaches t_c, Leyraz and Tschudi[22] conjectured that Smoluchowski's equation is satisfied

by

$$p(x,t) \propto x^{-\tau} \exp[-N_1(x(t_c - t)^{1/\sigma})^{\omega}] \tag{34}$$

Ernst et al.[21] showed that a general moment relation can be derived from eq 34.

$$p^{(n)} \approx B_n(t_c - t)^{-(n+1-\tau)/\sigma} \tag{35}$$

where B_n is a constant, $\tau = {}^3/_2 + \omega$, and $\sigma = \omega - {}^1/_2$. The critical exponent, γ, is then obtained by substituting $n = 2$ into eq 35

$$\gamma = \frac{\tau - 3}{\sigma} = \frac{{}^3/_2 - \omega}{\omega - {}^1/_2} \tag{36}$$

Substituting eq 35 back into the moment equations, we obtain the expression for the gel time t_c for an arbitrary ω

$$t_c = \frac{-\omega + {}^3/_2}{\omega - {}^1/_2} \frac{p^{(2)}(0)}{2\kappa[p^{(1+\omega)}(0)]^2} \tag{37}$$

The detailed deviation of t_c is presented in the Appendix.

In this paper we emphasize a numerical solution for the moment eqs 31−33 and compare the results with the analytical solutions for γ and t_c. In many cases the model for a real process is quite complex, involving other reactions such as propagation and/or a complicated reaction rate kernel that render analytical solutions impossible. The numerical approach has a wider application and, when the analytical approach fails, can provide solutions to most problems provided that an accurate third moment closure approximation is used. The numerical approach allows solutions for the zeroth, first, and second moment eqs 31−33. The total mass, $p^{(1)}$, is constant, and only two nonlinear ordinary differential equations need to be solved. The fractional moments $p^{(\omega)}$ and $p^{(1+\omega)}$ in eqs 15 and 17 are approximated from eq 20 (Γ closure) and eq 28 (log−normal closure), whose parameters are obtained from $n = 0$, 1, 2 moments. When ω is 0 or 1, $p^{(\omega)}$ and $p^{(1+\omega)}$ from eq 20 will be exact. The simulation results for the gel time (t_c) and the critical component (γ) for different ω values, as well as the analytical solutions, are shown in Table 1. The value of the gel time t_c depends on the

Table 1. Effect of ω on Cross-Linking Reactions

	exact solution[21]		Γ closure		log−normal closure	
ω	t_c	γ	t_c	γ	t_c	γ
1/3	∞	N/A	∞	N/A	∞	N/A
1/2	∞	N/A	1077	N/A	1.25×10^4	N/A
3/5	4.40	9	2.66	5.08	2197	N/A
0.65	2.57	5.67	1.62	3.35	4.82	13.5
2/3	2.21	5	1.42	3.05	3.28	9
3/4	1.16	3	0.82	2.02	1.17	3.3
4/5	0.83	7/3	0.62	1.70	0.79	2.25
5/6	0.67	2	0.52	1.53	0.63	1.89
1	0.25	1	0.25	1	0.25	1

initial conditions and on κ, but the slope γ is influenced only by ω. Gel forms only when ω is greater than a certain critical value, ω_c. For both closure approximations, Table 1 shows the minimum ω that allows gel to form ($\omega_c \approx {}^1/_2$), in agreement with the analysis of aggregation with similar kinetics.[20−24] The slope ($-\gamma$) increases with decreasing ω. Figures 2 and 3 show the

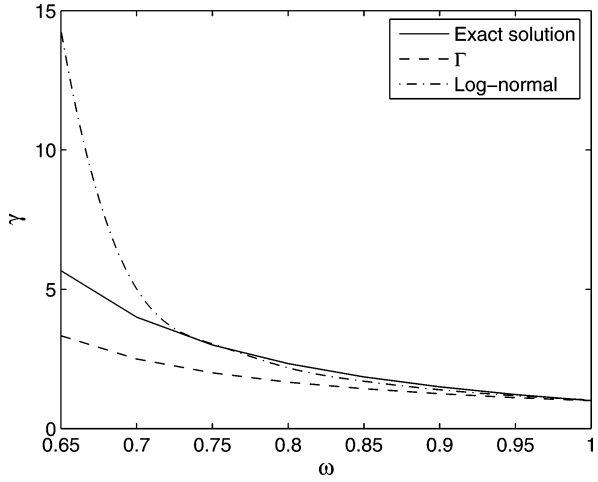

Figure 2. Comparison of analytical solution of γ with numerical solutions using Γ and log−normal closures.

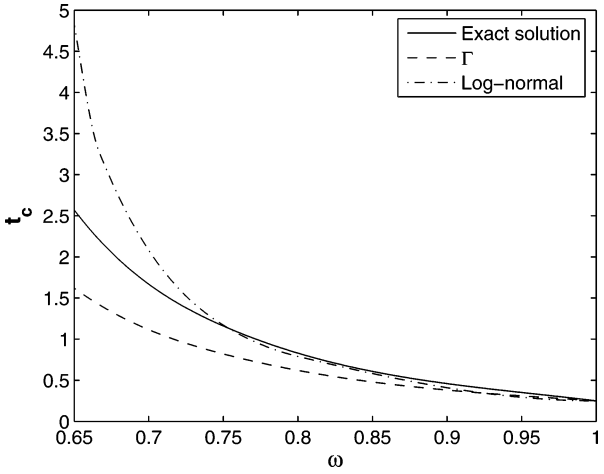

Figure 3. Comparison of analytical solution of t_c with numerical solutions using Γ and log−normal closures.

comparison of the analytical (exact) solution of γ and t_c vs ω with the approximated solution obtained from simulation using Γ and log−normal closures.

For γ (Figure 2) the two approximations have no noticeable errors when ω is close to 1, where the analytical solution yields $\gamma = 1$. When $\omega < 1$, the difference becomes more significant as ω decreases. The log−normal closure cannot produce the pronounced straight line segment (Figure 1) when $\omega < 0.62$, due to errors caused by the closure, which increase with decreasing ω. When ω is between 0.7 and 1, log−normal closure yields a better approximation than γ closure. Both approximations, however, show that ω in the range from ${}^2/_3$ to 1 yields γ values that include the experimentally observed values, 2.7 and 1.7 for polymer and silica systems. For instance, Γ closure predicts ω close to ${}^2/_3$ and ${}^3/_4$ to yield γ of 2.7 and 1.7, respectively. The log−normal closure predicts γ is 2.7 and 1.7 when ω is close to ${}^4/_5$ and ${}^5/_6$, respectively, and is closer to the exact values, 0.77 and 0.87, respectively. For t_c (Figure 3), a similar conclusion can also be obtained that when $0.7 < \omega \leq 1$, log−normal produces better predictions than Γ closure.

We can conclude that Γ closure underestimates γ when $\omega < 1$, while log−normal closure predicts a more accurate value of γ, which is overestimated for smaller ω. The true values for ω between ${}^1/_2$ and ${}^3/_4$ are bracketed by the solutions of Γ and log−normal ap-

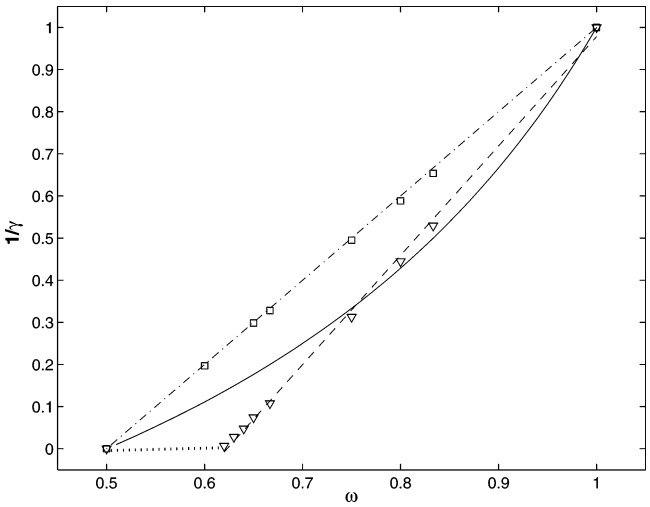

Figure 4. Computed values of $1/\gamma$ for various ω; the squares and triangles are Γ and log−normal closures, respectively; the solid line is the exact solution (based on eq 36), and dash−dot and dashed lines are eqs 38 and 39, respectively. The regressed lines have $r^2 = 0.9997$ for Γ closure and $r^2 = 0.998$ for log−normal closure ($\omega \geq 0.62$).

proximations and are closer to that of log−normal for larger ω and closer to Γ for smaller ω. This conclusion is similar to Papavasiliou et al.[15] for long chain branching of a free radical polymerization in a continuous stirred tank reactor (CSTR). For a given γ value, we may take as the approximated ω value the average of ω values for Γ and log−normal closures.

The obtained γ values in Table 1 are plotted as $1/\gamma$ vs ω in Figure 4. For the Γ closure, we find a linear relationship exists between $1/\gamma$ and ω

$$\frac{1}{\gamma} = 2.00(\omega - \omega_c) \tag{38}$$

represented by the regressed straight line (dash−dot) in Figure 4. The log−normal closure shows a linear relationship for $\gamma \geq 0.62$

$$\frac{1}{\gamma} = 2.59(\omega - 0.623) \tag{39}$$

This indicates the critical ω for log−normal closure is 0.623, an overestimate due to the large error of the log−normal closure when ω is smaller than one. The difficulty in identifying the slope $-\gamma$ suggests that $\omega_c = {}^1/_2$ is reached by the dashed line in Figure 4. It is, nevertheless, rather surprising that the linear relationships in Figure 4 are valid with excellent fits indicated by regression coefficients. The exact solution, shown as solid line in Figure 4, is not a straight line and is bracketed by the two closures for ω between ${}^1/_2$ and ${}^3/_4$, closer to log−normal closure for ω between ${}^3/_4$ and 1.

Although simulation results presented above cannot produce the exact ω values for the sol−gel transition of polymers and silica-based sol−gel, they show that ω is about ${}^3/_4$ for silica-based sol−gel and ${}^5/_6$ for polymers. This can also be explained qualitatively as follows. The rates of intermolecular cross-linking reactions are proportional to the number of functional groups in one polymer accessible to those of other polymers. If the polymer is uncoiled without any folding or entanglement, all the functional groups on the polymer are accessible. Thus, the number of accessible functional groups is proportional to its length or mass; in other words, $\omega = 1$. When polymer is contracted into a spherical shape, only the functional groups on the surface are accessible; thus, the number of accessible functional groups is proportional to its surface area. Because the polymer volume is proportional to its mass, the number of accessible functional groups is thus proportional to the ${}^2/_3$ power of its mass, or $\omega = {}^2/_3$. Under normal conditions, polymer chains fold and entangle, thus restricting access to some functional groups by other polymers. So for a real polymer system ω should be between ${}^2/_3$ and 1, in agreement with the value ($\sim{}^5/_6$) obtained from the proposed intermolecular cross-linking mechanism. Silica-based sol−gel reactions are more complicated because monomers added to the polymer restrict the access of unreacted monomers[27] (first shell substitution effects), resulting in smaller ω ($\sim{}^3/_4$) and thus larger γ.

Conclusion

The detailed quantitative description of the sol−gel critical transition is important for a fundamental understanding of polymer and gelation kinetics. In the present work we have shown how a population balance (distribution kinetics) approach handles this problem. A key element in the approach is to establish the intermolecular cross-linking mechanism, eq 2, and to write the population balance for the distribution, $p(x,t)$. Although we considered a general polycondensation process, eqs 6−8, the results show that only the cross-linking reaction influences the pregelation transition to the critical gel time. Focusing on the cross-linking kinetics and the exponent in the rate kernel expression, eq 3 allowed a generalization of the classic Flory−Stockmayer result, for which γ in eq 1 is 1. This procedure involved developing moment equations and a closure method to solve the differential equations. An analytical expression for t_c is obtained for the first time. A significant conclusion is that the exponent ω controls the slope γ of the sol−gel transition, while initial distribution and rate constant also control the gel time t_c. The Γ and log−normal distribution closure approximations bracket the values of γ and t_c, with log−normal a better approximation when $0.7 < \omega \leq 1$. They also provide unexpected linear relationships between $1/\gamma$ and ω. When $\omega = 1$, the classic result obtains, and when ω is either ${}^2/_3$ or ${}^3/_4$, good approximations to experimental values of γ for silica sol−gel or polymer, respectively, are found.

Appendix A. Derivation of Expression for the Critical Exponent

First rewrite eq 34 as

$$p(x,t) = N_2 x^{-\tau} \exp[-N_1(x(1 - t_c/t)^{1/\sigma})^{\omega}] \tag{40}$$

and substitute into the moment definition

$$p^{(n)}(t) = \int_{x=0}^{\infty} x^n p(x,n)\, dx \tag{41}$$

One obtains

$$p^{(n)}(t) = \frac{N_2}{\omega} {N_1}^{1+(1/2-n)/\omega} \Gamma\left(-1 + \frac{-{}^1/_2 + n}{\omega}\right) (1 - t/t_c)^{(\omega - n + 1/2)/(\omega - 1/2)} \tag{42}$$

and the critical exponent for nth moment ($n \geq 2$) is

$$\gamma_n = \frac{n - \omega - {}^1/_2}{\omega - {}^1/_2} \tag{43}$$

So the critical exponent for the weight-average molecular weight or the second moment is $({}^3/_2 - \omega)/(\omega - {}^1/_2)$.

Appendix B. Derivation of Expression for the Gel Time

In eq 42 define the constant $N[n] = (N_2/\omega)N_1^{1+(1/2-n)/\omega}\Gamma[-1 + (-{}^1/_2 + n)/\omega]$ and substitute eq 42 into the moment equation (see eq 14)

$$\frac{\mathrm{d}p^{(n)}}{\mathrm{d}t} = -2\kappa p^{(n+\omega)}p^{(\omega)} + \kappa\sum_{h=0}^{n}\binom{n}{h}p^{(\omega+h)}p^{(\omega+n-h)} \tag{44}$$

Because the power of $\mathrm{d}p^{(n)}/\mathrm{d}t$, $p^{(n+\omega)}p^{(\omega)}$, and $p^{(\omega+h)}p^{(\omega+n-h)}$ are all $(1 - t/t_c)^{(1-n)/(\omega-1/2)}$, we can collect the constant terms and obtain

$$\frac{N[n]}{-t_c}\frac{\omega - n + {}^1/_2}{\omega - {}^1/_2} = -2\kappa N[n+\omega]N[\omega] + \kappa\sum_{h=0}^{n}\binom{n}{h}N[h+\omega]N[n+\omega-h] \tag{45}$$

Therefore, we obtain t_c by letting $n = 2$

$$t_c = \frac{N[n]}{-2\kappa N[n+\omega]N[\omega] + \kappa\sum_{h=0}^{n}\binom{n}{h}N[h+\omega]N[n+\omega-h]\left.\frac{\omega + n - {}^1/_2}{\omega - {}^1/_2}\right|_{n=2}} \tag{46}$$

$$= \frac{N[2]}{2\kappa(N[1+\omega])^2}\frac{{}^3/_2 - \omega}{\omega - {}^1/_2} \tag{47}$$

$$= \frac{p^{(2)}(0)}{2\kappa[p^{(1+\omega)}(0)]^2}\frac{{}^3/_2 - \omega}{\omega - {}^1/_2} \tag{48}$$

For the special case $\omega = 1$, we obtain

$$t_c = \frac{1}{2\kappa p^{(2)}(0)} \tag{49}$$

The same solution obtained by solving the moment equations directly.

References and Notes

(1) Flory, P. J. *Principles of Polymer Chemistry;* Cornell University Press: Ithaca, NY, 1953.
(2) Stockmayer, W. H. *J. Chem. Phys.* **1943**, *11,* 45−55.
(3) Dotson, N. A.; Galvan, R.; Laurence, R. L.; Tirrell, M. *Polymerization Process Modeling;* VVCH Publishers: New York, 1996.
(4) Dotson, N. A.; Diekmann, T.; Macosko, C. W.; Tirrell, M. *Macromolecules* **1992**, *25,* 4490−4500.
(5) Martin, J. E.; Wilcoxon, J.; Adolf, D. *Phys. Rev. A* **1987**, *36,* 1803−1810.
(6) Winter, R.; Hua, D. W.; Song, X.; Mantulin, W.; Jonas, J. *J. Phys. Chem.* **1990**, *94,* 2706−2713.
(7) de Gennes, P. G. *Scaling Concepts in Polymer Physics;* Cornell University Press: Ithaca, NY, 1979.
(8) Manneville, P.; de Seze, L. In *Numerical Method in the Study of Critical Phenomena*; Della-Dora, I., Demongeot, J., Lacole, B., Eds.; Springer Press: Berlin, Germany, 1981.
(9) Herrmann, H. J.; Landau, D. P.; Stauffer, D. *Phys. Rev. Lett.* **1982**, *49,* 412−415.
(10) Pandey, R. B.; Liu, Y. *J. Sol.-Gel Sci. Technol.* **1999**, *15,* 147−159.
(11) Li, R.; McCoy, B. J. *Macromol. Theory Simul.* **2004**, *13,* 203−218.
(12) Brinker, C. J.; Scherer, G. W. *Sol−Gel Science: The Physics and Chemistry of Sol−Gel Processing;* Academic Press: San Diego, CA, 1990.
(13) Li, R.; McCoy, B. J. *Macromol. Rapid Commun.* **2004**, *25,* 1059−1063.
(14) Teymour, F.; Campbell, J. D. *Macromolecules* **1994**, *27*, 2460−2469.
(15) Papavasiliou, G.; Birol, I.; Teymour, F. *Macromol. Theory Simul.* **2002**, *11,* 533−548.
(16) Li, R.; Corripio, A. B.; Dooley, K. M.; Henson, M. A.; Kurtz, M. J. *Chem. Eng. Sci.* **2004**, *51,* 2297−2313.
(17) Frenklach, M. *Chem. Eng. Sci.* **2002**, *57,* 2229−2239.
(18) Diemer, R. B.; Olson, J. H. *Chem. Eng. Sci.* **2002**, *57,* 2211−2228.
(19) McGraw, R. *Aerosol Sci. Technol.* **1997**, *27,* 255−265.
(20) Ziff, R. M.; Hendriks, E. M.; Ernst, M. H. *Phys. Rev. Lett.* **1982**, *49,* 593−595.
(21) Ernst, M. H.; Hendriks, E. M.; Ziff, R. M. *J. Phys. A: Math. Gen.* **1982**, *15,* L743−L747.
(22) Leyvraz, F.; Tschudi, H. R. *J. Phys. A: Math. Gen.* **1982**, *15,* 1951−1964.
(23) Leyvraz, F. *J. Phys. A: Math. Gen.* **1983**, *16,* 2861−2873.
(24) Leyvraz, F. *Phys. Rep.* **2003**, *383,* 95−212.
(25) Scott, W. T. *J. Atmos. Sci.* **1968**, *25,* 54−65.
(26) Ziff, R. M.; Ernst, M. H.; Hendriks, E. M. *J. Phys. A: Math. Gen.* **1983**, *16,* 2293−2320.
(27) Rankin, S. E.; Kasehagen, L. J.; McCormick, A. V.; Macosko, C. W. *Macromolecules* **2000**, *33,* 7639−7648.

MA050707B